

ALPHA DECAY

Alpha particles were first identified as the least penetrating of the radiations emitted by naturally occurring materials. In 1903, Rutherford measured their charge-to-mass ratio by deflecting α particles from the decay of radium in electric and magnetic fields. Despite the difficulty of these early experiments, Rutherford's result was only about 25% higher than the presently accepted value. In 1909 Rutherford showed that, as suspected, the α particles were in fact helium nuclei; in his experiments the particles entered an evacuated thin-walled chamber by penetrating its walls, and after several days of collecting, atomic spectroscopy revealed the presence of helium gas inside the chamber.

Many heavy nuclei, especially those of the naturally occurring radioactive series, decay through α emission. Only exceedingly rarely does any other spontaneous radioactive process result in the emission of nucleons; we do not, for example, observe deuteron emission as a natural decay process. There must therefore be a special reason that nuclei choose α emission over other possible decay modes. In this chapter we examine this question and study the α decay process in detail. We also show how α spectroscopy can help us to understand nuclear structure.

8.1 WHY α DECAY OCCURS

Alpha emission is a Coulomb repulsion effect. It becomes increasingly important for heavy nuclei because the disruptive Coulomb force increases with size at a faster rate (namely, as Z^2) than does the specific nuclear binding force, which increases approximately as A .

Why is the α particle chosen as the agent for the spontaneous carrying away of positive charge? When we call a process *spontaneous* we mean that some kinetic energy has suddenly appeared in the system for no apparent cause; this energy must come from a decrease in the mass of the system. The α particle, because it is a very stable and tightly bound structure, has a relatively small mass compared with the mass of its separate constituents. It is particularly favored as an emitted particle if we hope to have the disintegration products as light as possible and thus get the largest possible release of kinetic energy.

Table 8.1 Energy Release (Q value) for Various Modes of Decay of $^{232}\text{U}^a$

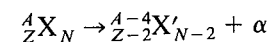
Emitted Particle	Energy Release (MeV)	Emitted Particle	Energy Release (MeV)
n	-7.26	^4He	+5.41
^1H	-6.12	^5He	-2.59
^2H	-10.70	^6He	-6.19
^3H	-10.24	^6Li	-3.79
^3He	-9.92	^7Li	-1.94

^aComputed from known masses.

For a typical α emitter ^{232}U (72 y) we can compute, from the known masses, the energy release for various emitted particles. Table 8.1 summarizes the results. Of the particles considered, spontaneous decay is energetically possible *only* for the α particle. A positive disintegration energy results for some slightly heavier particles than those listed, ^8Be or ^{12}C , for example. We will show, however (Section 8.4), that the partial disintegration constant for emission of such heavy particles is normally vanishingly small compared with that for α emission. Such decays would be so rare that in practice they would almost never be noticed. This suggests that if a nucleus is to be recognized as an alpha emitter it is not enough for α decay to be energetically possible. The disintegration constant must also not be too small or else α emission will occur so rarely that it may not be detected. With present techniques this means that the half-life must be less than about 10^{16} y. Also, β decay, if it has a much higher partial disintegration constant, can mask the α decay. Most nuclei with $A > 190$ (and many with $150 < A < 190$) are energetically unstable against α emission but only about one-half of them can meet these other requirements.

8.2 BASIC α DECAY PROCESSES

The spontaneous emission of an α particle can be represented by the following process:



The α particle, as was shown by Rutherford, is a nucleus of ^4He , consisting of two neutrons and two protons. To understand the decay process, we must study the conservation of energy, linear momentum, and angular momentum.

Let's first consider the conservation of energy in the α decay process. We assume the initial decaying nucleus X to be at rest. Then the energy of the initial system is just the rest energy of X, $m_X c^2$. The final state consists of X' and α , each of which will be in motion (to conserve linear momentum). Thus the final total energy is $m_{X'} c^2 + T_{X'} + m_\alpha c^2 + T_\alpha$, where T represents the kinetic energy of the final particles. Thus conservation of energy gives

$$m_X c^2 = m_{X'} c^2 + T_{X'} + m_\alpha c^2 + T_\alpha \quad (8.1)$$

or

$$(m_X - m_{X'} - m_\alpha) c^2 = T_{X'} + T_\alpha \quad (8.2)$$

The quantity on the left side of Equation 8.2 is the net energy released in the decay, called the Q value:

$$Q = (m_X - m_{X'} - m_\alpha)c^2 \quad (8.3)$$

and the decay will occur spontaneously only if $Q > 0$. (The decay Q values for ^{232}U were listed in Table 8.1.) Q values can be calculated from atomic mass tables because even though Equation 8.3 represents a nuclear process, the electron masses will cancel in the subtraction. When the masses are in atomic mass units (u), expressing c^2 as 931.502 MeV/u gives Q values directly in MeV.

The Q value is also equal to the total kinetic energy given to the decay fragments:

$$Q = T_{X'} + T_\alpha \quad (8.4)$$

If the original nucleus X is at rest, then its linear momentum is zero, and conservation of linear momentum then requires that X' and α move with equal and opposite momenta in order that the final momentum also be zero:

$$p_\alpha = p_{X'} \quad (8.5)$$

α decays typically release about 5 MeV of energy. Thus for both X' and α , $T \ll mc^2$ and we may safely use nonrelativistic kinematics. Writing $T = p^2/2m$ and using Equations 8.4 and 8.5 gives the kinetic energy of the α particle in terms of the Q value:

$$T_\alpha = \frac{Q}{(1 + m_\alpha/m_{X'})} \quad (8.6)$$

Because the mass ratio is small compared with 1 (recall that X' represents a heavy nucleus), it is usually sufficiently accurate to express this ratio simply as $4/(A - 4)$, which gives, with $A \gg 4$,

$$T_\alpha = Q(1 - 4/A) \quad (8.7)$$

Typically, the α particle carries about 98% of the Q value, with the much heavier nuclear fragment X' carrying only about 2%. (This recoil energy of the heavy fragment is not entirely negligible. For a typical Q value of 5 MeV, the recoiling nucleus has an energy of the order of 100 keV. This energy is far in excess of that which binds atoms in solids, and thus the recoiling nucleus, if it is near the surface of the radioactive source, escapes from the source and can spread to the surroundings. If the α decay is part of a decay chain, then the recoiling daughter nucleus may itself be radioactive, and these recoils can result in the spread of radioactive material. Fortunately, the heavy recoil nuclei have an extremely short range in matter and their spread can be prevented by a thin coating, such as Mylar or lacquer, placed over the radioactive sample.)

The kinetic energy of an α particle can be measured directly with a magnetic spectrometer, and so the Q value of a decay can be determined. This gives us a way to determine atomic masses, such as in a case in which we might know the mass of long-lived X as a result of direct measurement but X' is so short-lived that its mass cannot be determined by direct measurement.

8.3 α DECAY SYSTEMATICS

One feature of α decay is so striking that it was noticed as long ago as 1911, the year that Rutherford "discovered" the nucleus. Geiger and Nuttall noticed that α emitters with large disintegration energies had short half-lives and conversely. The variation is astonishingly rapid as we may see from the limiting cases of ^{232}Th (1.4×10^{10} y; $Q = 4.08$ MeV) and ^{218}Th (1.0×10^{-7} s; $Q = 9.85$ MeV). A factor of 2 in energy means a factor of 10^{24} in half-life! The theoretical explanation of this Geiger-Nuttall rule in 1928 was one of the first triumphs of quantum mechanics.

A plot of $\log t_{1/2}$ against Q in which all α emitters are included shows a considerable scatter about the general Geiger-Nuttall trend. Very smooth curves result, however, if we plot only α emitters with the same Z and if further we select from this group only those with Z and N both even (Figure 8.1). Even-odd, odd-even, and odd-odd nuclei obey the general trend but do not plot into quite such smooth curves; their periods are 2–1000 times longer than those for even-even types with the same Z and Q .

It is interesting that ^{235}U (even Z , odd N) is one of these "extra-long-life" types. If its half-life were 1000 times shorter, this important nucleus would not occur in nature, and we probably would not have nuclear reactors today! We see in Chapter 13 that the same feature that apparently accounts for the long life against α decay, namely the odd neutron, also makes ^{235}U very susceptible to fission by thermal neutrons.

Figure 8.2 shows another important systematic relationship for α emitters. Looking for the moment only at the data for $A > 212$, we see that adding neutrons to a nucleus reduces the disintegration energy, which, because of the

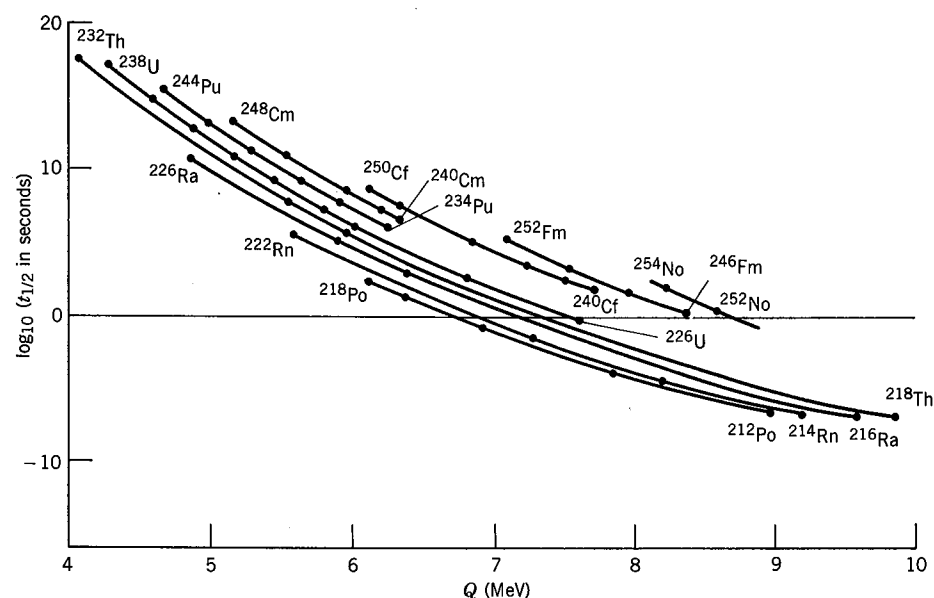


Figure 8.1 The inverse relationship between α -decay half-life and decay energy, called the Geiger-Nuttall rule. Only even- Z , even- N nuclei are shown. The solid lines connect the data points.

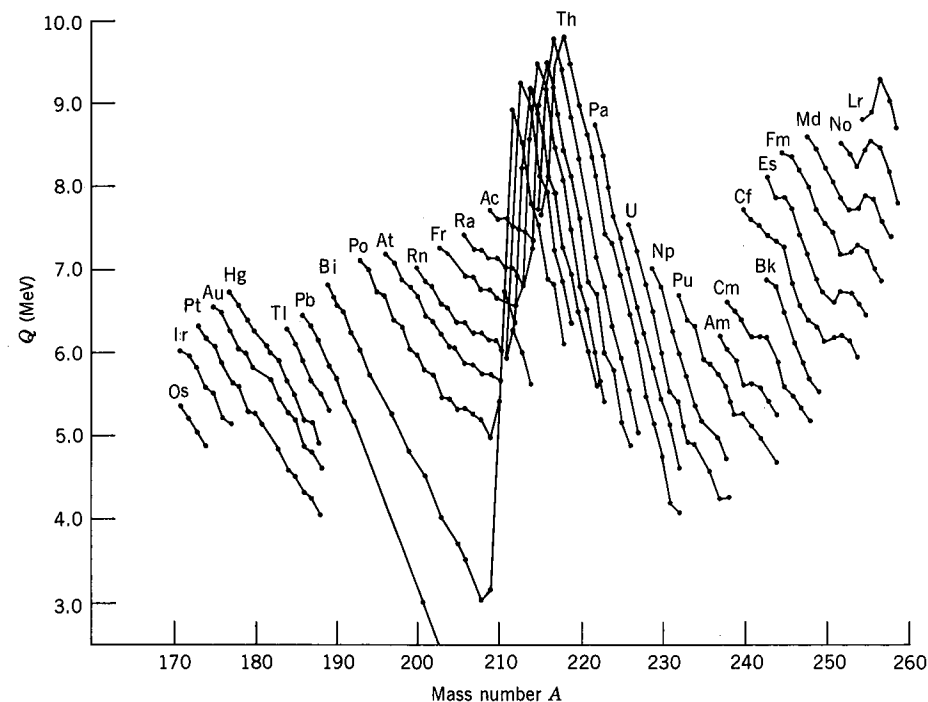


Figure 8.2 Energy released in α decay for various isotopic sequences of heavy nuclei. In contrast to Figure 8.1, both odd- A and even- A isotopes are shown, and a small amount of odd-even staggering can be seen. The effects of the shell closures at $N = 126$ (large dip in data) and $Z = 82$ (larger than average spacing between Po, Bi, and Pb sequences) are apparent.

Geiger-Nuttall rule, increases the half-life. The nucleus becomes more stable. A striking discontinuity near $A = 212$ occurs where $N = 126$ and is another example of nuclear shell structure.

We can compare the systematic dependence of Q on A with the prediction of the semiempirical mass formula, Equation 3.28.

$$Q = B(^4\text{He}) + B(Z - 2, A - 4) - B(Z, A) \quad (8.8)$$

$$\begin{aligned} &\cong 28.3 - 4a_v + \frac{8}{3}a_s A^{-1/3} + 4a_c Z A^{-1/3} (1 - Z/3A) \\ &\quad - 4a_{\text{sym}} (1 - 2Z/A)^2 + 3a_p A^{-7/4} \end{aligned} \quad (8.9)$$

where the approximation in Equation 8.9 is $Z, A \gg 1$. For ^{226}Th , this formula gives $Q = 6.75$ MeV, not too far from the measured value of 6.45 MeV. What is perhaps more significant is that the general trend of Figure 8.2 is reproduced: for ^{232}Th , Equation 8.9 gives $Q = 5.71$ MeV (to be compared with $Q = 4.08$ MeV), while for ^{220}Th the formula gives $Q = 7.77$ MeV (compared with $Q = 8.95$ MeV). Keep in mind that the parameters of the semiempirical mass formula are chosen to give rough agreement with observed binding energies across the entire range of nuclei. It is important that the formula gives us rough agreement with the decay Q values and that it correctly gives $Q > 0$ for the heavy nuclei. It also

correctly predicts the decrease of Q with increasing A for a sequence of isotopes such as those of thorium, although it gives too small a change of Q with A (the formula gives $\Delta Q = -0.17$ MeV per unit change in A , while for Th the observed average change is $\Delta Q = -0.40$ MeV per unit change in A).

8.4 THEORY OF α EMISSION

The general features of Figure 8.1 can be accounted for by a quantum mechanical theory developed in 1928 almost simultaneously by Gamow and by Gurney and Condon. In this theory an α particle is assumed to move in a spherical region determined by the *daughter* nucleus. The central feature of this *one-body model* is that the α particle is preformed inside the parent nucleus. Actually there is not much reason to believe that α particles do exist separately within heavy nuclei; nevertheless, the theory works quite well, especially for even-even nuclei. This success of the theory does not prove that α particles are preformed, but merely that they behave as if they were.

Figure 8.3 shows a plot, suitable for purposes of the theory, of the potential energy between the α particle and the residual nucleus for various distances between their centers. The horizontal line Q is the disintegration energy. Note that the Coulomb potential is extended inward to a radius a and then arbitrarily cut off. The radius a can be taken as the sum of the radius of the residual nucleus and of the α particle. There are three regions of interest. In the spherical region $r < a$ we are inside the nucleus and speak of a potential well of depth $-V_0$, where V_0 is taken as a positive number. Classically the α particle can move in this region, with a kinetic energy $Q + V_0$ but it cannot escape from it. The annular-shell region $a < r < b$ forms a potential barrier because here the potential energy

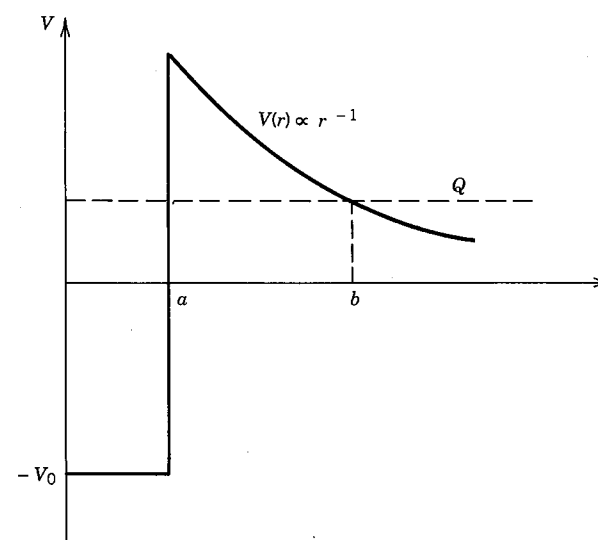


Figure 8.3 Relative potential energy of α -particle, daughter-nucleus system as a function of their separation. Inside the nuclear surface at $r = a$, the potential is represented as a square well; beyond the surface, only the Coulomb repulsion operates. The α particle tunnels through the Coulomb barrier from a to b .

is more than the total available energy Q . Classically the α particle cannot enter this region from either direction, just as a tennis ball dropped from a certain height cannot rebound higher; in each case the kinetic energy would have to be negative. The region $r > b$ is a classically permitted region outside the barrier.

From the classical point of view, an α particle in the spherical potential well would sharply reverse its motion every time it tried to pass beyond $r = a$. Quantum mechanically, however, there is a chance of "leakage" or "tunnelling" through such a barrier. This barrier accounts for the fact that α -unstable nuclei do not decay immediately. The α particle within the nucleus must present itself again and again at the barrier surface until it finally penetrates. In ^{238}U , for example, the leakage probability is so small that the α particle, on the average, must make $\sim 10^{38}$ tries before it escapes ($\sim 10^{21}$ per second for $\sim 10^9$ years)!

The barrier also operates in reverse, in the case of α -particle scattering by nuclei (see Sections 3.1 and 11.6). Alpha particles incident on the barrier from outside the nucleus usually scatter in the Coulomb field if the incident energy is well below the barrier height. Tunnelling through the barrier, so that the nuclear force between the particle and target can cause nuclear reactions, is a relatively improbable process at low energy. The theoretical analysis of nuclear reactions induced by charged particles uses a formalism similar to that of α decay to calculate the barrier penetration probability. Fusion reactions, such as those responsible for the energy released in stars, also are analyzed using the barrier penetration approach (see Section 14.2).

The disintegration constant of an α emitter is given in the one-body theory by

$$\lambda = fP \quad (8.10)$$

where f is the frequency with which the α particle presents itself at the barrier and P is the probability of transmission through the barrier.

Equation 8.10 suggests that our treatment is going to be semiclassical in that our discussion of the situation for $r < a$ is very "billiard-ballish." A rigorous wave-mechanical treatment, however, gives about the same results for this problem. The quantity f is roughly of the order of v/a where v is the relative velocity of the α particle as it rattles about inside the nucleus. We can find v from the kinetic energy of the α particle for $r < a$. Estimating $V_0 \approx 35$ MeV for a typical well depth gives $f \approx 6 \times 10^{21}/\text{s}$ for $Q \approx 5$ MeV. We will see later that we do not need to know f very precisely to check the theory.

The barrier penetration probability P must be obtained from a quantum mechanical calculation similar to the one-dimensional problem discussed in Section 2.3. Let's first use the result of that calculation, Equation 2.39, to estimate the probability P . Of course, the calculation that led to Equation 2.39 was based on a one-dimensional rectangular barrier, which is not directly applicable to the $1/r$ Coulomb potential, but we can at least find a rough order-of-magnitude estimate. The result, Equation 2.39, depends on the width of the barrier and on its height (called V_0 for the rectangular barrier) above the energy E of the particle. The Coulomb barrier of Figure 8.3 has height B at $r = a$, where

$$B = \frac{1}{4\pi\epsilon_0} \frac{zZ'e^2}{a} \quad (8.11)$$

In this expression the α particle has charge ze and the daughter nucleus, which

provides the Coulomb repulsion, has charge $Z'e = (Z - z)e$. The height of the barrier thus varies from $(B - Q)$ above the particle's energy at $r = a$ to zero at $r = b$, and we can take a representative average height to be $\frac{1}{2}(B - Q)$. We can similarly choose a representative average width to be $\frac{1}{2}(b - a)$. The factor k_2 of Equation 2.39 then becomes $\sqrt{(2m/\hbar^2) \cdot \frac{1}{2}(B - Q)}$. For a typical heavy nucleus ($Z = 90$, $a = 7.5$ fm), the barrier height B is about 34 MeV, so the factor k_2 is about 1.6 fm^{-1} . The radius b at which the α particle "leaves" the barrier is found from the equality of the particle's energy and the potential energy:

$$b = \frac{1}{4\pi\epsilon_0} \frac{zZ'e^2}{Q} \quad (8.12)$$

and for a typical case of a heavy nucleus with $Q \approx 6$ MeV, $b \approx 42$ fm. Thus $k_2 \cdot \frac{1}{2}(b - a) \gg 1$ and we can approximate Equation 2.39 as

$$P \approx e^{-2k_2 \cdot (1/2)(b-a)} \quad (8.13)$$

since the factors in front of the exponential are of unit order of magnitude. For the case we are estimating here, $P \sim 2 \times 10^{-25}$ and thus $\lambda \sim 10^{-3}/\text{s}$ and $t_{1/2} \sim 700$ s. A slight change of Q to 5 MeV changes P to 1×10^{-30} and $t_{1/2} \sim 10^8$ s. Even this very crude calculation is able to explain the many orders of magnitude change of $t_{1/2}$ between $Q = 5$ MeV and $Q = 6$ MeV, as illustrated in Figure 8.1.

The exact quantum mechanical calculation is very similar in spirit to the crude estimate above. We can think of the Coulomb barrier as made up of a sequence of infinitesimal rectangular barriers of height $V(r) = zZ'e^2/4\pi\epsilon_0 r$ and width dr . The probability to penetrate each infinitesimal barrier, which extends from r to $r + dr$, is

$$dP = \exp\left\{-2 dr \sqrt{(2m/\hbar^2)[V(r) - Q]}\right\} \quad (8.14)$$

The probability to penetrate the complete barrier is

$$P = e^{-2G} \quad (8.15)$$

where the *Gamow factor* G is

$$G = \sqrt{\frac{2m}{\hbar^2}} \int_a^b [V(r) - Q]^{1/2} dr \quad (8.16)$$

which can be evaluated as

$$G = \sqrt{\frac{2m}{\hbar^2 Q}} \frac{zZ'e^2}{4\pi\epsilon_0} \left[\arccos \sqrt{x} - \sqrt{x(1-x)} \right] \quad (8.17)$$

where $x = a/b = Q/B$. The quantity in brackets in Equation 8.17 is approximately $\pi/2 - 2x^{1/2}$ when $x \ll 1$, as is the case for most decays of interest. Thus the result of the quantum mechanical calculation for the half-life of α decay is

$$t_{1/2} = 0.693 \frac{a}{c} \sqrt{\frac{mc^2}{2(V_0 + Q)}} \exp\left\{2 \sqrt{\frac{2mc^2}{(\hbar c)^2 Q}} \frac{zZ'e^2}{4\pi\epsilon_0} \left(\frac{\pi}{2} - 2\sqrt{\frac{Q}{B}}\right)\right\} \quad (8.18)$$

Table 8.2 Calculated α -Decay Half-lives for Th Isotopes

A	Q (MeV)	$t_{1/2}$ (s)	
		Measured	Calculated
220	8.95	10^{-5}	3.3×10^{-7}
222	8.13	2.8×10^{-3}	6.3×10^{-5}
224	7.31	1.04	3.3×10^{-2}
226	6.45	1854	6.0×10^1
228	5.52	6.0×10^7	2.4×10^6
230	4.77	2.5×10^{12}	1.0×10^{11}
232	4.08	4.4×10^{17}	2.6×10^{16}

The results of this calculation for the even isotopes of Th are shown in Table 8.2. The agreement is not exact, but the calculation is able to reproduce the trend of the half-lives within 1–2 orders of magnitude over a range of more than 20 orders of magnitude. We have neglected several important details in the calculation: we did not consider the initial and final nuclear wave functions (Fermi's Golden Rule, Equation 2.79, must be used to evaluate the decay probability), we did not consider the angular momentum carried by the α particle, and we assumed the nucleus to be spherical with a mean radius of $1.25A^{1/3}$ fm. The latter approximation has a very substantial influence on the calculated half-lives. The nuclei with $A \geq 230$ have strongly deformed shapes, and the calculated half-lives are extremely sensitive to small changes in the assumed mean radius. For instance, changing the mean radius to $1.20A^{1/3}$ (a 4% change in a) changes the half-lives by a factor of 5! In fact, because of this extreme sensitivity, the procedure is often reversed—the measured half-lives are used to deduce the nuclear radius; what actually comes out of the calculation is more like the sum of the radii of the nucleus X' and the α particle, if we assume their charge distributions to have a sharp edge. This result can then be used to obtain an estimate of the nuclear radius; see, for example, L. Marquez, *J. Phys. Lett.* **42**, 181 (1981).

Even though this oversimplified theory is not strictly correct, it gives us a good estimate of the decay half-lives. It also enables us to understand why other decays into light particles are not commonly seen, even though they may be allowed by the Q value. For example, the decay $^{220}\text{Th} \rightarrow ^{12}\text{C} + ^{208}\text{Po}$ would have a Q value of 32.1 MeV, and carrying through the calculation using Equation 8.18 gives $t_{1/2} = 2.3 \times 10^6$ s for the ^{220}Th decay into ^{12}C . This is a factor of 10^{13} longer than the α -decay half-life and thus the decay will not easily be observable.

Recently, just such a decay mode has in fact been observed, the first example of a spontaneous decay process involving emission of a particle heavier than an α . The decay of ^{223}Ra normally proceeds by α emission with a half-life of 11.2 d, but there has now been discovered the decay process $^{223}\text{Ra} \rightarrow ^{14}\text{C} + ^{209}\text{Pb}$. The probability for this process is very small, about 10^{-9} relative to the α decay. Figure 8.4 indicates the heroic efforts that are necessary to observe the process. To confirm that the emitted particle is ^{14}C requires the $\Delta E \cdot T$ technique discussed in Chapter 7. Figure 8.4 shows a portion of the high-energy end of the tail of the hyperbola expected for observation of carbon. From the mass tables,

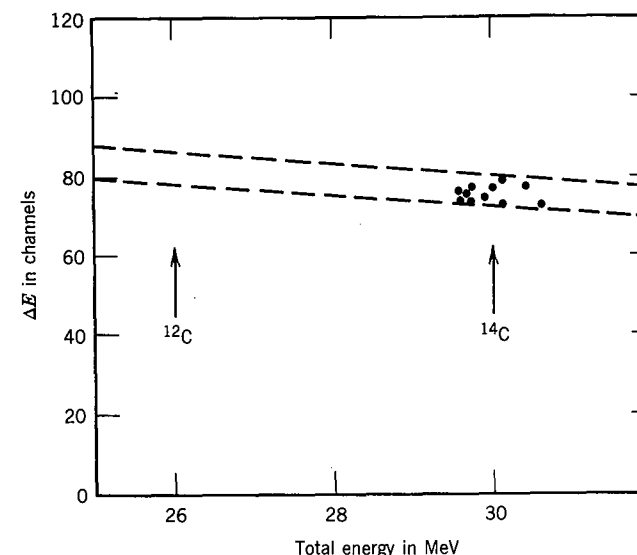


Figure 8.4 A portion of the tail of the $\Delta E \cdot T$ hyperbola showing the observed ^{14}C events from the decay of ^{223}Ra . The dashed lines show the limits expected for carbon. The 11 ^{14}C events result from 6 months of counting. From H. J. Rose and G. A. Jones, *Nature* **307**, 245 (1984). Reprinted by permission, copyright © Macmillan Journals Limited.

the decay Q value is calculated to be 31.8 MeV, which (when corrected for the recoil) gives a ^{14}C kinetic energy of 29.8 MeV. By contrast, the calculated energy for ^{12}C emission would be about 26 MeV. The total of 11 events observed represents about *six months* of counting with a source of $3.3 \mu\text{Ci}$ of ^{223}Ra in secular equilibrium with 21-y ^{227}Ac , a member of the naturally occurring actinium series beginning with ^{235}U .

Calculating the Gamow factor for ^{14}C emission gives a decay probability of about 10^{-3} relative to α emission; the discrepancy between the calculated and observed (10^{-9}) values results from the assumptions about the preformation of the particle inside the nucleus. You will recall that our theory of α decay is based on the assumption that the α is preformed inside the nucleus. What the experiment tells us is that the probability for forming ^{14}C clusters inside the nucleus is about 10^{-6} relative to the probability to preform α 's.

For a description of the experiment, see H. J. Rose and G. A. Jones, *Nature* **307**, 245 (1984). Emission of ^{14}C from several other nuclei in this region has also been observed, and emission of heavier decay fragments, including ^{24}Ne , has been reported.

Going in the opposite direction, we can use Equation 8.18 with $z = 1$ to evaluate the half-life for proton decay—that is, the spontaneous emission of a proton by an unstable nucleus. In this case the Coulomb barrier will be only half as high as it is for α decay, but these decays are inhibited for a stronger reason: the Q values for proton decay are generally negative and so the decays are absolutely forbidden by energy conservation. Such decays have recently been observed for a few proton-rich unstable nuclei, which are formed in nuclear reactions by bombarding a target with $N \approx Z$ using a projectile having $N \approx Z$.

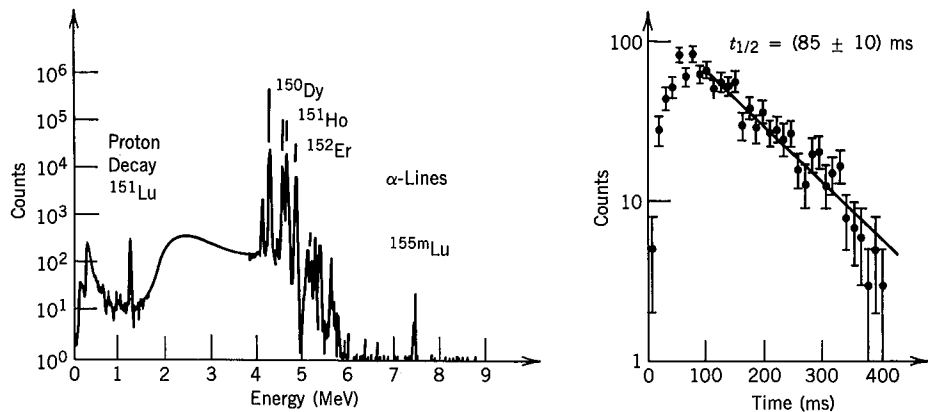


Figure 8.5 (Left) Charged-particle spectrum emitted in the radioactive decays of products of the reaction $^{96}\text{Ru} + ^{58}\text{Ni}$. The peaks above 4 MeV represent α decays; the 1.2-MeV peak is from proton emission. (Right) The decay with time of the proton peak gives a half-life of 85 ms. From S. Hofmann et al., *Z. Phys. A* **305**, 111 (1982).

This creates a heavy nucleus with $N \approx Z$, a very unstable configuration, and proton emission may be energetically possible, as the nucleus tries to relieve itself of its proton excess. The Q value for proton decay can be found by a slight modification of Equation 8.3, which gives exactly the negative of the proton separation energy, Equation 3.27. Proton decay will be energetically possible when the Q value is positive and therefore when the separation energy is negative. A glance at the mass tabulations (see A. H. Wapstra and G. Audi, *Nucl. Phys. A* **432**, 1 (1985)) shows only a few very rare cases in which the proton separation energy is negative, and even these are not directly measured but instead obtained by extrapolations from more stable nuclei.

In an experiment reported by Hofmann et al., *Z. Phys. A* **305**, 111 (1982), a target of ^{96}Ru was bombarded with ^{58}Ni projectiles. Figure 8.5 shows the spectrum of light particles emitted following the reaction. The more energetic peaks are identified as α decays from unstable nuclei in the neighborhood of $A = 150$ produced in the reaction. The peak at 1.239 MeV was identified as a proton using $\Delta E \cdot T$ techniques as described in Chapter 7. Its half-life was measured as 85 ms, as shown in Figure 8.5. The decay was assigned to the isotope ^{151}Lu based on a series of indirect arguments; unfortunately, reactions such as this produce many different products, and it is often a difficult task to identify the source of the observed radiations. This experiment thus provides evidence for the decay $^{151}\text{Lu} \rightarrow ^{150}\text{Yb} + \text{p}$.

Study of decays such as this enables us to extend our knowledge of nuclear mass systematics far beyond the previous limits; for instance, at the time of this work ^{151}Lu was three protons further from stability than the previous last known isobar (^{151}Er). Figure 8.6 shows the Q_p values deduced from known masses and from extrapolations based on systematics. The value for ^{151}Lu lies right on the theoretical calculation, giving confidence to both the identification of the isotope and to the theoretical calculation.

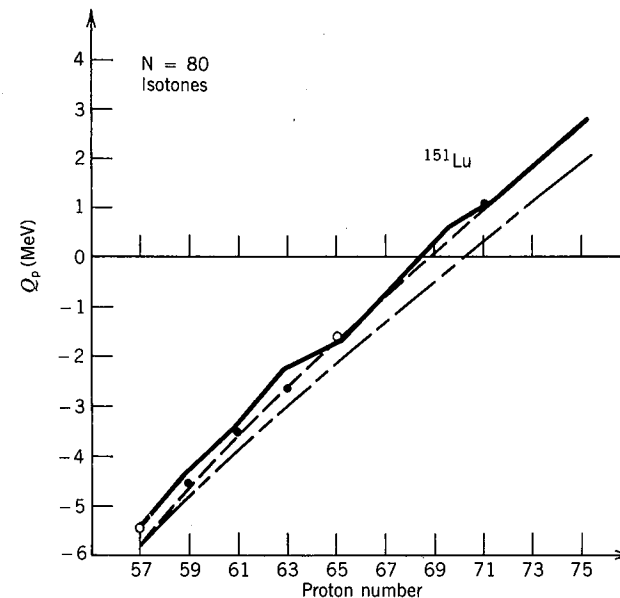


Figure 8.6 Proton-decay energies of $N = 80$ isotones. The solid lines are theoretical calculations based on nuclear mass formulas (somewhat like the semiempirical mass formula). Only for ^{151}Lu is the decay energy positive. From S. Hofmann et al., *Z. Phys. A* **305**, 111 (1982).

Using Equation 8.18 for the half-life gives a value of about $1.7 \mu\text{s}$, too small by nearly 5 orders of magnitude. For this reason, it has been proposed that the decay is inhibited by differences in the nuclear structure of the initial and final states (or possibly by a large angular momentum change in the decay, examples of which are discussed in the next section).

8.5 ANGULAR MOMENTUM AND PARITY IN α DECAY

We have up to this point neglected to discuss the angular momentum carried by the α particle. In a transition from an initial nuclear state of angular momentum I_i to a final state I_f , the angular momentum of the α particle can range between $I_i + I_f$ and $|I_i - I_f|$. The nucleus ^4He consists of two protons and two neutrons, all in 1s states and all with their spins coupled pairwise to 0. The spin of the α particle is therefore zero, and the total angular momentum carried by an α particle in a decay process is purely orbital in character. We will designate this by ℓ_α . The α particle wave function is then represented by a $Y_{\ell m}$ with $\ell = \ell_\alpha$; thus the parity change associated with α emission is $(-1)^{\ell_\alpha}$, and we have a parity selection rule, indicating which transitions are permitted and which are absolutely forbidden by conservation of parity: if the initial and final parities are the same, then ℓ_α must be even; if the parities are different, then ℓ_α must be odd.

To study the applications of these rules, we must recognize that we have also neglected one very significant feature of α decay—a given initial state can populate many different final states in the daughter nucleus. This property is

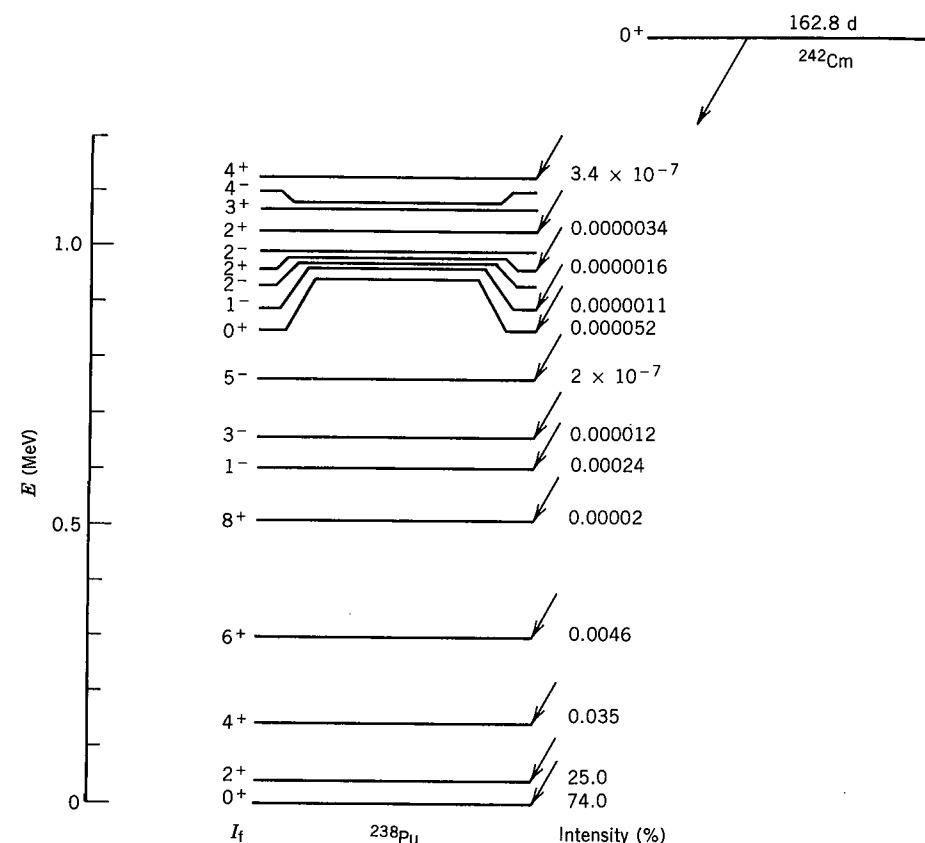


Figure 8.7 α decay of ^{242}Cm to different excited states of ^{238}Pu . The intensity of each α -decay branch is given to the right of the level.

sometimes known as the “fine structure” of α decay, but of course has nothing whatever to do with atomic fine structure. Figure 8.7 shows the α decay of ^{242}Cm . The initial state is spin zero, and thus the angular momentum of the α particle ℓ_α is equal to the angular momentum of the final nuclear state I_f . You can see that many different states of ^{238}Pu are populated. The α decays have different Q values (given by the Q value for decay to the ground state, 6.216 MeV, less the excitation energy of the excited state) and different intensities. The intensity depends on the wave functions of the initial and final states, and also depends on the angular momentum ℓ_α . In Equation 2.60, it was shown how the “centrifugal potential” $\ell(\ell+1)\hbar^2/2mr^2$ must be included in spherical coordinates. This term, which is always positive, has the effect of raising the potential energy for $a < r < b$ and thus increasing the thickness of the barrier which must be penetrated. Consider for example the 0^+ , 2^+ , 4^+ , 6^+ , and 8^+ states of the ground-state rotational band. The decay to the 2^+ state has less intensity than the decay to the ground state for two reasons—the “centrifugal potential” raises the barrier by about 0.5 MeV, and the excitation energy lowers Q by 0.044 MeV. The decay intensity continues to decrease for these same reasons as we go up the band to the 8^+ state. If we use our previous theory for the decay rates, taking

into account the increasing effective B and decreasing Q , we obtain the following estimates for the relative decay branches: 0^+ , 76%; 2^+ , 23%; 4^+ , 1.5%; 6^+ , 0.077%; 8^+ , $8.4 \times 10^{-5}\%$. These results are not in exact agreement with the observed decay intensities, but they do give us a rough idea of the origin of the decrease in intensity.

Once we go above the ground-state band, the α decay intensities become very small, of the order of $10^{-6}\%$ of the total decay intensity. This situation results from the poor match of initial and final wave functions—many of these excited states originate with vibrations or pair-breaking particle excitations, which are not at all similar to the paired, vibrationless 0^+ ground state of ^{242}Cm . You should note that there are some states for which there is no observed decay intensity at all. These include the 2^- states at 0.968 and 0.986 MeV, the 3^+ state at 1.070 MeV, and the 4^- state at 1.083 MeV. Alpha decay to these states is absolutely forbidden by the parity selection rule. For example, a $0 \rightarrow 3$ decay must have $\ell_\alpha = 3$, which must give a change in parity between initial and final states. Thus $0^+ \rightarrow 3^-$ is possible, but not $0^+ \rightarrow 3^+$. Similarly, $0 \rightarrow 2$ and $0 \rightarrow 4$

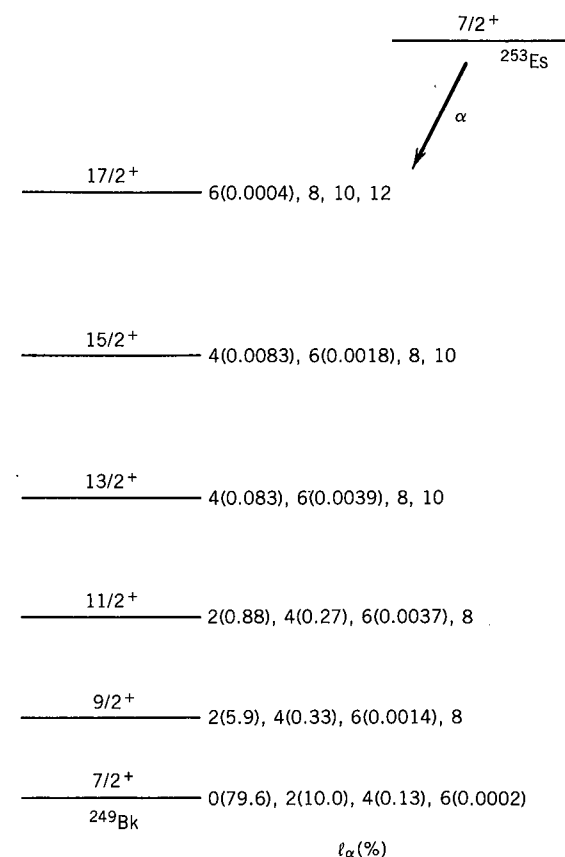


Figure 8.8 Intensities of various α -decay angular momentum components in the decay of ^{253}Es . For $\ell_\alpha = 8$ and higher, the intensities are not known but are presumably negligibly small. From the results of a study of spin-aligned α decays by A. J. Soinski et al., *Phys. Rev. C* 2, 2379 (1970).

decays cannot change the parity, and so $0^+ \rightarrow 2^-$ and $0^+ \rightarrow 4^-$ are not permitted.

When neither the initial nor the final states have spin 0, the situation is not so simple and there are no absolutely forbidden decays. For example, the decay $2^- \rightarrow 2^+$ must have odd ℓ_α (because of the change in parity), and the angular momentum coupling rules require $0 \leq \ell_\alpha \leq 4$. Thus it is possible to have this decay with $\ell_\alpha = 1$ or 3. The next question that occurs is whether $\ell_\alpha = 1$ or $\ell_\alpha = 3$ is favored and by how much. Our previous discussion would lead us to guess that the $\ell_\alpha = 1$ intensity is roughly an order of magnitude greater than the $\ell_\alpha = 3$ intensity. However, measuring only the energy or the intensity of the decay gives us no information about how the total decay intensity is divided among the possible values of ℓ_α . To make the determination of the relative contributions of the different ℓ values, it is necessary to measure the angular distribution of the α particles. The emission of an $\ell = 1$ α particle is governed by a $Y_1(\theta, \phi)$, while an $\ell = 3$ α decay is emitted with a distribution according to $Y_3(\theta, \phi)$. If we determine the spatial distribution of these decays, we could in principle determine the relative amounts of the different ℓ values.

To do this experiment we must first align the spins of our α -radioactive nuclei, such as by aligning their magnetic dipole or electric quadrupole moments in a magnetic field or in a crystalline electric field gradient. Keeping the spins aligned requires that the nuclei must be cooled to a temperature at which the thermal motion is not sufficient to destroy the alignment; generally temperatures below 0.01 K are required (that is, less than 0.01 degree above the absolute zero of temperature!).

As an example of such an experiment, we consider the decay of ^{253}Es to states of the ground-state rotational band of ^{249}Bk . The possible ℓ values are indicated in Figure 8.8, and the results of measuring the α -particle angular distributions help us to determine the relative contribution of the different values of ℓ_α .

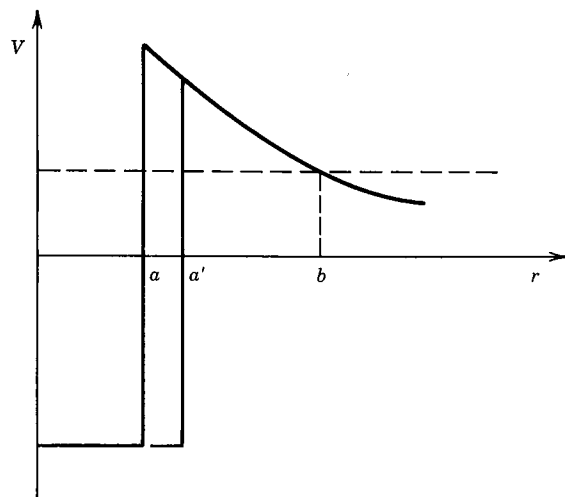


Figure 8.9 In a deformed nucleus, α particles escaping from the poles enter the Coulomb barrier at the larger separation a' , and must therefore penetrate a lower, thinner barrier. It is therefore more probable to observe emission from the poles than from the equator.

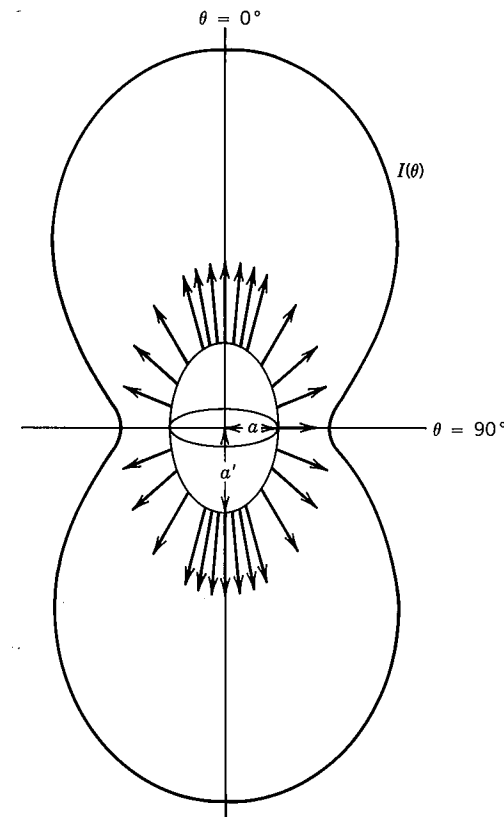


Figure 8.10 Intensity distribution of α particles emitted from the deformed nucleus at the center of the figure. The polar plot of intensity shows a pronounced angular distribution effect.

Since many α -emitting nuclei are deformed, these angular distribution measurements can also help us to answer another question: if we assume a stable prolate (elongated) nucleus, will more α 's be emitted from the poles or from the equator? Figure 8.9 suggests a possible answer to this question: at the larger radius of the poles, the α particle feels a weaker Coulomb potential and must therefore penetrate a thinner and lower barrier. We therefore expect that polar emission ought to be more likely than equatorial emission. Figure 8.10 shows the angular distribution of α emission relative to the symmetry axis. You can see that emission from the poles is 3–4 times more probable than emission from the equator, exactly as we expect on the basis of the potential.

8.6 α DECAY SPECTROSCOPY

The final topic in our discussion of α decay is this: What can we learn about the energy levels of nuclei by studying α decay?

Let's consider, for example, the 5.3-h decay of ^{251}Fm to levels of ^{247}Cf . (The levels of ^{247}Cf are also populated in the beta decay of ^{247}Es , but the half-life of that decay is so short, 4.7 min, that it is more difficult to use as a detailed probe of the level structure of ^{247}Cf .)

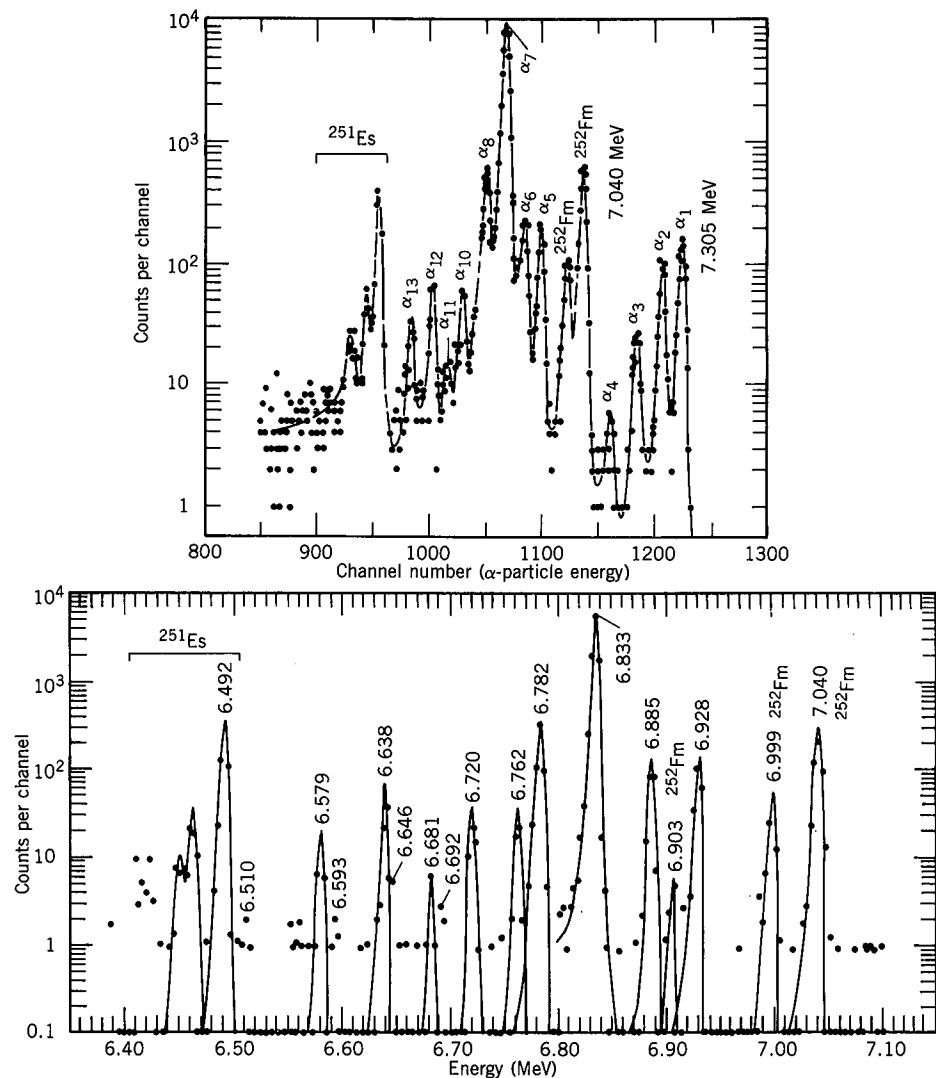


Figure 8.11 α spectrum from the decay of ^{251}Fm . The top portion shows the spectrum as observed with a Si detector. The bottom shows a portion of the same spectrum observed with a magnetic spectrometer, whose superior energy resolution enables observation of the 6.762-MeV decay, which would be missed in the upper spectrum. From Ahmad et al., *Phys. Rev. C* **8**, 737 (1973).

Figure 8.11 shows the energy spectrum of α decays from the decay of ^{251}Fm . As you can see, there are 13 distinct groups of α particles; each group presumably represents the decay to a different excited state of ^{247}Cf . How can we use this information to construct the level scheme of ^{247}Cf ? Based on the α spectrum, we first must find the energy and intensity of each α group. The energy is found by comparing with decays of known energy (the impurity decays from the ^{252}Fm contaminant are helpful for this) and the intensity is found from the area of each peak. The result of this analysis is shown in Table 8.3, along with the uncertainties that come mostly from the counting statistics for each peak. (Notice that the

Table 8.3 α Decays from ^{251}Fm

α Group	α Energy (keV)	Decay Energy (keV)	Excited-State Energy (keV)	α Intensity (%)
α_1	7305 ± 3	7423	0	1.5 ± 0.1
α_2	7251 ± 3	7368	55	0.93 ± 0.08
α_3	7184 ± 3	7300	123	0.29 ± 0.03
α_4	7106 ± 5	7221	202	~ 0.05
α_5	6928 ± 2	7040	383	1.8 ± 0.1
α_6	6885 ± 2	6996	427	1.7 ± 0.1
α_7	6833 ± 2	6944	479	87.0 ± 0.9
α_8	6782 ± 2	6892	531	4.8 ± 0.2
α_9	6762 ± 3	6872	552	0.38 ± 0.06
α_{10}	6720 ± 3	6829	594	0.44 ± 0.04
α_{11}	6681 ± 4	6789	634	0.07 ± 0.03
α_{12}	6638 ± 3	6745	678	0.56 ± 0.06
α_{13}	6579 ± 3	6686	738	0.26 ± 0.04

strongest peaks have the smallest *relative* uncertainties.) To find the decay energies (that is, the relative energies of the nuclear states), we must use Equation 8.7, since the measured α energies are only the kinetic energies. These are also shown in Table 8.3.

The different ^{247}Cf excited states will quickly decay to the ground state by emitting γ -ray photons, so in constructing the decay scheme it is helpful to have the energies and intensities of the γ rays as well. Figure 8.12 shows the observed γ rays and Table 8.4 shows the deduced energies and intensities.

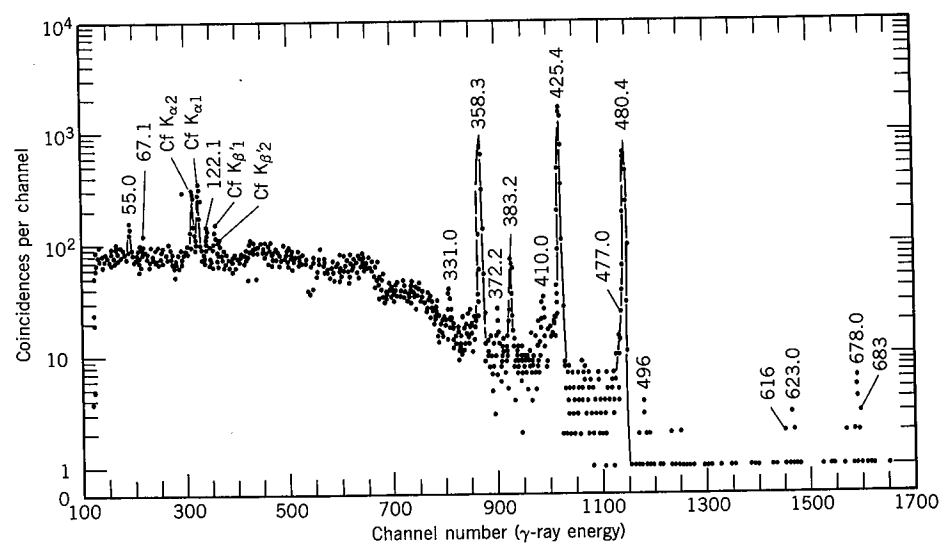


Figure 8.12 γ -ray spectrum of ^{251}Fm in coincidence with all α decays in the range 6.0 to 7.7 MeV. The spectrum was obtained with a Ge(Li) detector.

Table 8.4 γ Rays in ^{247}Cf following α Decay of ^{251}Fm

Energy (keV)	Intensity (% of decays)	Energy (keV)	Intensity (% of decays)
55.0 \pm 0.2	0.58 \pm 0.08	425.4 \pm 0.1	51 \pm 4
67.1 \pm 0.2	0.28 \pm 0.05	477.0 \pm 0.3	0.54 \pm 0.08
122.1 \pm 0.2	0.28 \pm 0.05	480.4 \pm 0.1	21 \pm 2
331.0 \pm 0.3	0.35 \pm 0.07	496 \pm 1	\sim 0.08
358.3 \pm 0.1	17 \pm 1.5	616 \pm 1	\sim 0.05
372.2 \pm 0.4	0.25 \pm 0.05	623.0 \pm 0.8	0.07 \pm 0.02
382.2 \pm 0.3	1.2 \pm 0.13	678.0 \pm 0.8	0.26 \pm 0.06
410.0 \pm 0.3	0.50 \pm 0.07	683 \pm 1	\sim 0.04

Now the detective work comes. Let's assume (and here we must be very careful, as we see in the next example) that the highest energy α decay populates the ground state of ^{247}Cf . (In an even-even nucleus, this would be a very good assumption, because $0^+ \rightarrow 0^+$ α decays are very strong and not inhibited by any differences between the wave functions of the initial and final nuclear states. In an odd- A nucleus, the initial and final ground states may have very different characters so that the decay to the ground state may be very weak or even vanishing.) The decay just lower in energy differs from the ground-state decay by about 55 keV. Assuming this to populate the first excited state, we are pleased to find among the γ transitions one of energy 55 keV, which presumably represents the transition between the first excited state and the ground state. The next α decay populates a state at 123 ± 3 keV above the ground state, and we find among the γ rays one of energy 122.1 keV, which corresponds to a transition from the second excited state to the ground state. We also find a transition of energy 67.1 (= 122.1 - 55.0) keV, which results from transitions between the second and first excited states.

Let's guess that these three states (with assumed energies 0, 55.0 keV, 122.1 keV) form a rotational band whose states, we recall from the discussion of odd- A deformed nuclei in Section 5.3, have angular momenta $I = \Omega, \Omega + 1, \Omega + 2, \dots$, where Ω is the component of the angular momentum of the odd particle along the symmetry axis. The energy difference between the first excited state and ground state should then be

$$\begin{aligned} \Delta E_{21} \equiv E_2 - E_1 &= \frac{\hbar^2}{2\mathcal{I}} [(\Omega + 1)(\Omega + 2) - \Omega(\Omega + 1)] \\ &= \frac{\hbar^2}{2\mathcal{I}} 2(\Omega + 1) \end{aligned} \quad (8.19)$$

where we have used $E = (\hbar^2/2\mathcal{I})I(I + 1)$ for the energy of rotational states. Similarly, the difference between the ground state and second excited state is

$$\begin{aligned} \Delta E_{31} \equiv E_3 - E_1 &= \frac{\hbar^2}{2\mathcal{I}} [(\Omega + 2)(\Omega + 3) - \Omega(\Omega + 1)] \\ &= \frac{\hbar^2}{2\mathcal{I}} 2(2\Omega + 3) \end{aligned} \quad (8.20)$$

Combining these results with the experimental values, $\Delta E_{21} = 55.0$ keV and $\Delta E_{31} = 122.1$ keV, we conclude $\Omega = 3.5 \pm 0.2$ (that is, $\Omega = \frac{7}{2}$) and $\hbar^2/2\mathcal{I} = 6.11 \pm 0.02$ keV. These three states thus seem to form a rotational band with $I = \frac{7}{2}, \frac{9}{2}, \frac{11}{2}$. With our deduced values we can predict the energy of the $\frac{13}{2}$ state:

$$\Delta E_{41} = \frac{\hbar^2}{2\mathcal{I}} \left[\frac{13}{2} \cdot \frac{15}{2} - \frac{7}{2} \cdot \frac{9}{2} \right] = 201.6 \text{ keV}$$

and the $\frac{15}{2}$ state

$$\Delta E_{51} = \frac{\hbar^2}{2\mathcal{I}} \left[\frac{15}{2} \cdot \frac{17}{2} - \frac{7}{2} \cdot \frac{9}{2} \right] = 293.3 \text{ keV}$$

Apparently, the $\frac{13}{2}$ state is populated by the very weak α_4 decay, but its γ decays may be too weak to be seen in the spectrum of Figure 8.12. The decay to the $\frac{15}{2}$ state is not observed.

The interpretation of the remaining states is aided by α - γ coincidence studies, in which we electronically select only those γ transitions that follow a given α decay within a certain short time interval (in this case 110 ns). Since this time is long compared with typical lifetimes of nuclear states, all γ rays that follow the α decay will be recorded, even those that follow indirectly (such as the case in which two γ 's are emitted in cascade, one following the other). The following coincidence relationships were observed:

Coincidence Gate	γ Rays (keV)
α_5	383.2
α_6	372.2, 383.2
α_7	55.0, 67.1, 122.1, 358.3, 425.4, 480.4
α_8	331.0, 358.3, 410.0, 425.4, 477.0, 480.4
α_{12}	623.0, 678.0

The decay α_5 goes to a state at 383.2 keV, which then goes directly to the ground state by emitting a single γ ray. The decay α_6 populates a state at about 427 keV. There is no coincident γ ray of that energy, which indicates no direct transition to the ground state, but there is a transition of energy 372.2 keV which, when added to 55.0 keV, gives 427.2 keV, very close to the energy of the state. We therefore conclude that this state, at 427.2 keV, decays to the first excited state at 55.0 keV. There is also a coincident transition at 383.2 keV, and thus this state at 427.2 keV must decay to the previously established state at 383.2 keV, by emitting a γ ray of energy $427.2 - 383.2 = 44.0$ keV; this γ ray is not observed. The decay α_7 to the state at 480.4 keV shows decays to the ground state and to the 55.0 and 122.1 keV states ($425.4 + 55.0 = 480.4$; $358.3 + 122.1 = 480.4$). Similarly, the decay α_8 to a state of 532.0 keV shows direct transitions to the lower states ($331.0 + 201.0 = 532.0$; $410.0 + 122.1 = 532.1$; $477.0 + 55.0 = 532.0$) but not directly to the ground state. It also shows coincident transitions that originate from the 480.4-keV level, so there must be a transition of energy 51.6 keV (= $532.0 - 480.4$). In a similar fashion we analyze the other α and γ decays, and Figure 8.13 shows the resulting decay scheme.

For the states above the ground-state band, the assignment of spins and intrinsic angular momentum Ω is not as easy as it was for the states of the

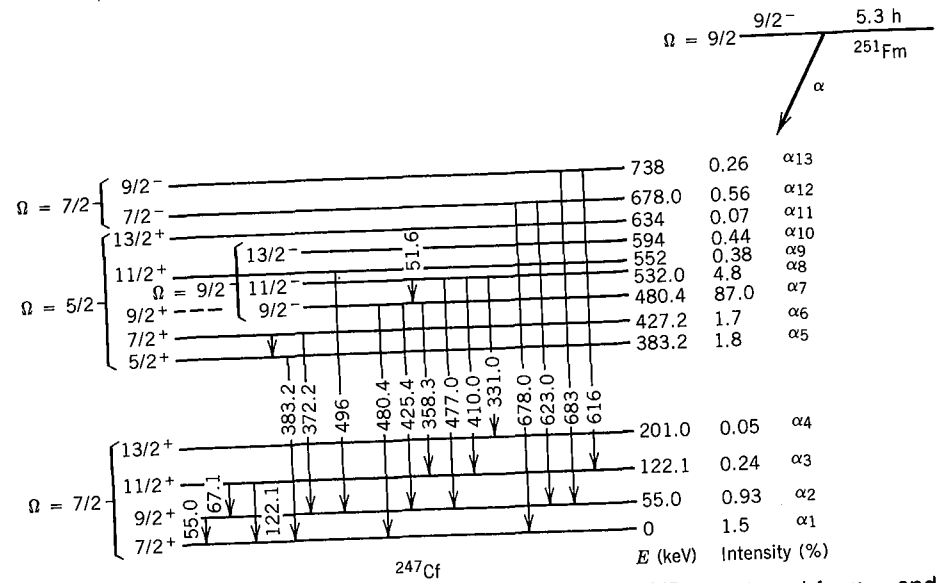


Figure 8.13 The decay scheme of ^{251}Fm to levels of ^{247}Cf deduced from α and γ spectroscopy. The spin assignments for the higher levels are deduced using γ -ray and internal conversion techniques described in Chapter 10.

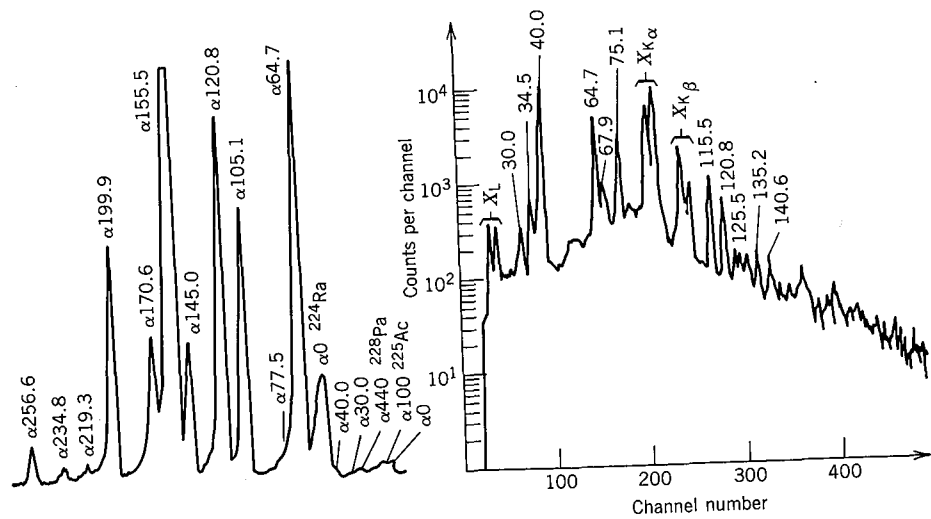


Figure 8.14 α (left) and γ (right) spectra from the decay of ^{229}Pa to ^{225}Ac . The α peaks are labeled according to the excited state populated in ^{225}Ac ; thus $\alpha_{105.1}$ indicates the decay leading to the excited state at 105.1 keV. Prominent peaks from impurities are also indicated. The γ spectrum is taken in coincidence with all α 's. From P. Aguer et al., *Nucl. Phys. A* **202**, 37 (1973).

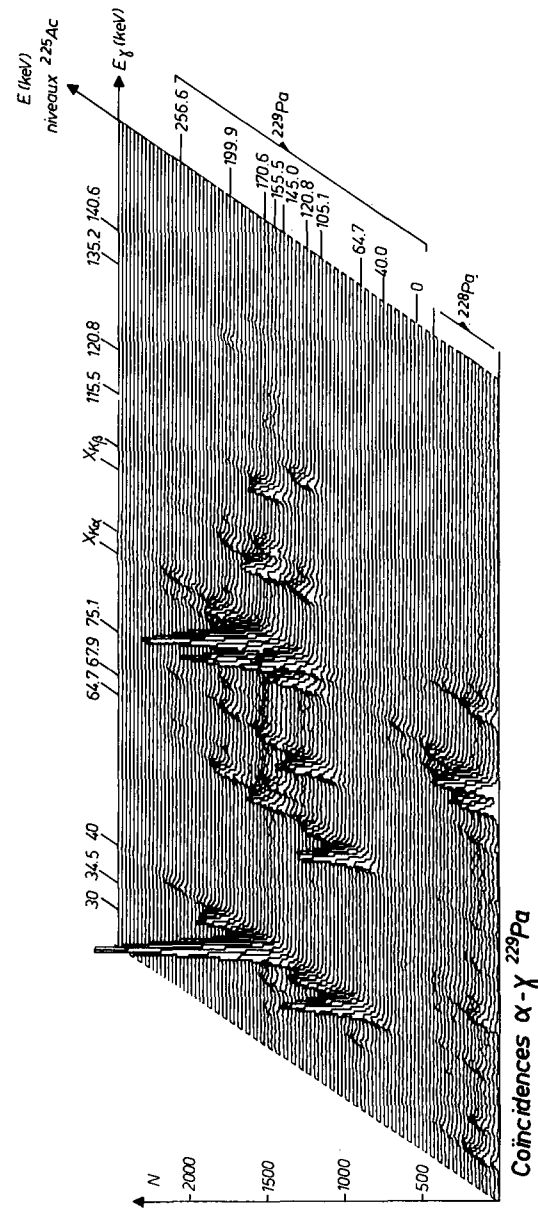


Figure 8.15 Three-dimensional (sometimes called two-parameter) representation of α - γ coincidences in the decay of ^{229}Pa . The horizontal axis shows γ -ray energies, labeled along the top. The oblique axis gives the α -decay energies, labeled to indicate the ^{225}Ac state populated in the decay. The vertical axis gives the intensity of the coincidence relationship.

ground-state rotational band. To make these assignments, we need additional information from the γ decays; these measurements are discussed in Chapter 10.

Notice the strong α branch to the state at 480.4 keV. This occurs because the wave functions of the initial and final states are identical—both come from the same $\Omega = \frac{5}{2}$ deformed single-particle state—and the result is that more than 93% of the decay intensity goes to states of that so-called “favored” band. The observed decay rates can be compared with values calculated for various deformed single-particle states using the Nilsson wave functions, and in general there is good agreement between the measured and calculated results, both for the favored and unfavored decays. It is such comparisons between theory and experiment that allow us to assign the single-particle states because the intrinsic Ω and Nilsson assignments are not directly measurable.

The data for this discussion were taken from I. Ahmad, J. Milsted, R. K. Sjoblom, J. Lerner, and P. R. Fields, *Phys. Rev. C* **8**, 737 (1973). Theoretical calculations of α transition amplitudes for states in even- A and odd- A deformed nuclei of the actinide region can be found in J. K. Poggenburg, H. J. Mang, and J. O. Rasmussen, *Phys. Rev.* **181**, 1697 (1969).

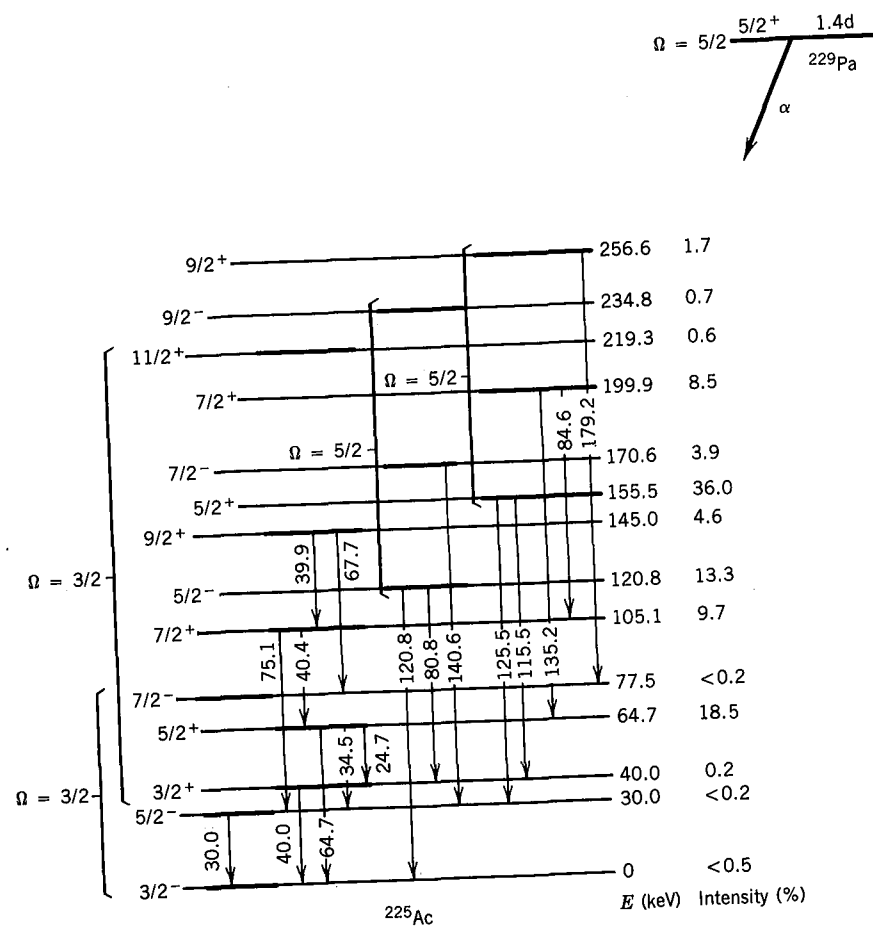


Figure 8.16 Decay scheme of ^{229}Pa deduced from α and γ spectroscopy.

Another example of the study of nuclear spectroscopy through α decay is illustrated in Figures 8.14–8.16. Figure 8.14 shows the α and γ spectra from the decay $^{229}\text{Pa} \rightarrow ^{225}\text{Ac}$, and you can see that the decay to the ground state (labeled α_0) cannot be verified. Again, the α - γ coincidences help to elucidate the decay scheme, and a particularly instructive way to illustrate the coincidences is shown in Figure 8.15. Each peak in this three-dimensional spectrum represents a definite coincidence relationship between the α and the γ that label the axes. The information derived from the coincidence studies is used to make the decay scheme shown in Figure 8.16. Four rotational bands are identified in ^{225}Ac , positive and negative parity bands with $\Omega = \frac{3}{2}$ and $\frac{5}{2}$. The decaying ^{229}Pa is assigned $\frac{5}{2}^+$, so in this case the favored decay to the $\frac{5}{2}^+$ band in the daughter has about 46% of the decay intensity. The decay to the $\frac{5}{2}^-$ ground-state rotational band is strongly inhibited by the nuclear wave functions, resulting in the very weak (and possibly nonexistent) decay to the ground state. In this case it would lead to errors if we had assumed that the highest energy observed α group ($\alpha_{64.7}$, or $\alpha_{40.0}$ if we looked carefully) corresponded to transitions to the ground state.

The data for the ^{229}Pa decay come from P. Aguer, A. Peghaire, and C. F. Liang, *Nucl. Phys. A* **202**, 37 (1973).

REFERENCES FOR ADDITIONAL READING

Somewhat more extensive discussions of α decay can be found in Chapter 16 of R. D. Evans, *The Atomic Nucleus* (New York: McGraw-Hill, 1955), and in Chapter 13 of I. Kaplan, *Nuclear Physics* (Reading, MA: Addison-Wesley, 1955). For surveys of α -decay theory, see H. J. Mang, *Ann. Rev. Nucl. Sci.* **14**, 1 (1964), and J. O. Rasmussen, “Alpha Decay,” in *Alpha-, Beta- and Gamma-Ray Spectroscopy*, edited by K. Siegbahn (Amsterdam: North-Holland, 1965), Chapter XI. A discussion of the use of α decay for nuclear spectroscopy is that of F. S. Stephens, in *Nuclear Spectroscopy*, part A, edited by F. Ajzenberg-Selove (New York: Academic, 1959), Section I.E.2.

PROBLEMS

- Find the Q values of the following decays:
 - $^{247}\text{Bk} \rightarrow ^{243}\text{Am} + \alpha$;
 - $^{251}\text{Cf} \rightarrow ^{247}\text{Cm} + \alpha$;
 - $^{230}\text{Th} \rightarrow ^{226}\text{Ra} + \alpha$.
- For each decay given in Problem 1, calculate the kinetic energy and velocity of the daughter nucleus after the decay.
- From the known atomic masses, compute the Q values of the decays:
 - $^{242}\text{Pu} \rightarrow ^{238}\text{U} + \alpha$
 - $^{208}\text{Po} \rightarrow ^{204}\text{Pb} + \alpha$
 - $^{208}\text{Po} \rightarrow ^{196}\text{Pt} + ^{12}\text{C}$
 - $^{210}\text{Bi} \rightarrow ^{208}\text{Pb} + ^2\text{H}$
- In the decay of ^{242}Cm to ^{238}Pu , the maximum α energy is 6112.9 ± 0.1 keV. Given the mass of ^{238}Pu , find the mass of ^{242}Cm .
- The highest energy α particle emitted in the decay of ^{238}U to ^{234}Th is 4196 ± 4 keV. From this information and the known mass of ^{238}U , compute the mass of ^{234}Th .

6. Use the uncertainty principle to estimate the minimum speed and kinetic energy of an α particle confined to the interior of a heavy nucleus.
7. (a) Compute the Q values for the decays $^{224}\text{Ra} \rightarrow ^{212}\text{Pb} + ^{12}\text{C}$ and $^{224}\text{Ra} \rightarrow ^{210}\text{Pb} + ^{14}\text{C}$. (b) Estimate the half-lives for these two possible decay processes. ^{224}Ra is an α emitter with a half-life of 3.66 days.
8. The Q value for the α decay of ^{203}Tl is calculated to be 0.91 MeV from the masses of the initial and final nuclei. Estimate the half-life of ^{203}Tl and explain why we call ^{203}Tl a "stable" nucleus.
9. Use the semiempirical mass formula to estimate the α -decay energy of ^{242}Cf and compare with the measured value (see Figure 8.1).
10. For the α decay of ^{226}Ra to ^{222}Rn ($Q = 4.869$ MeV), compute the expected half-lives for values of the ^{222}Rn radius of 7.0, 8.0, 9.0, and 10.0 fm. Estimate the nuclear radius required to give the measured half-life (1602 years); deduce the corresponding value of R_0 and interpret.
11. Using a scale similar to that of Figure 8.2, plot Equation 8.9 and show that it reproduces the general trend of the Q values. Choose appropriate values of Z corresponding to each A .
12. Make a drawing to scale of the Coulomb potential barrier encountered in the α decay of ^{242}Cm ($Z = 96$) to ^{238}Pu ($Z = 94$), for which $Q = 6.217$ MeV. Assume $R_0 = 1.5$ fm, to account for the diffuseness of the nuclear surface. Show also the Coulomb-plus-centrifugal barrier for the $\ell = 2$ decay to the first excited state (44 keV). Now use a method analogous to that of Equation 8.13 to estimate the reduction in the decay probability caused by the additional barrier, and correspondingly estimate the ratio of the α branching intensities to the ground and first excited states of ^{238}Pu . (Don't forget to reduce the Q value for decays to the excited state.) Compare your estimate with the actual intensities given in Figure 8.7.
13. Equations 8.1 to 8.5 are strictly correct even using relativistic mechanics; however, Equations 8.6 and 8.7 were obtained by assuming a nonrelativistic form for the kinetic energy. Using relativistic expressions for p and T , derive relativistic versions of Equations 8.6 and 8.7 and calculate the error made by neglecting these corrections for a 6-MeV α particle.
14. Consider the strongly distorted nucleus ^{252}Fm with $\epsilon = 0.3$. That is, the nucleus is shaped like an ellipsoid of revolution with semimajor axis $a' = R(1 + \epsilon)$ and semiminor axis $a = R(1 + \epsilon)^{-1/2}$, where R is the mean radius. Using a potential of the form of Figure 8.9, estimate the relative probabilities of polar and equatorial emission of α particles.
15. In a semiclassical picture, an $\ell = 0$ α particle is emitted along a line that passes through the center of the nucleus. (a) How far from the center of the nucleus must $\ell = 1$ and $\ell = 2$ α particles be emitted? Assume $Q = 6$ MeV for a heavy nucleus ($A = 230$). (b) What would be the recoil rotational kinetic energy if all of the recoil went into rotational motion of the daughter nucleus?
16. Use data from available reference material (*Table of Isotopes, Atomic Mass Tables*) to plot a series of curves showing α -decay Q values against Z for constant A . Use Equation 8.9 to analyze the graph.
17. In the decay $^{228}\text{Th} \rightarrow ^{224}\text{Ra} + \alpha$, the highest energy α particle has an energy 5.423 MeV and the next highest energy is 5.341 MeV. (a) The highest energy decay populates the ^{224}Ra ground state. Why is it natural to expect this to be so? (b) Compute the Q value for the decay from the measured α energy. (c) Compute the energy of the first excited state of ^{224}Ra .
18. The Q value of the decay $^{233}\text{U} \rightarrow ^{229}\text{Th} + \alpha$ is 4.909 MeV. Excited states of ^{229}Th at 29, 42, 72, and 97 keV are populated in the decay. Compute the energies of the five most energetic α groups emitted in the ^{233}U decay.
19. The five highest energy α 's emitted by ^{242}Cm (Figure 8.7) have energies (in MeV) of 6.113, 6.070, 5.972, 5.817, 5.609. Each state is connected with the state directly below it by a γ transition. Calculate the energies of the γ rays.
20. The α decay of a nucleus near mass 200 has two components of energies 4.687 and 4.650 MeV. Neither populates the ground state of the daughter, but each is followed by a γ ray, of respective energy 266 and 305 keV. No other γ rays are seen. (a) From this information, construct a decay scheme. (b) The decaying parent state has spin 1 and negative parity, and the ground state of the daughter has spin zero and also negative parity. Explain why there is no direct α decay to the ground state.
21. The α decay of ^{244}Cm populates a 0^+ excited state in ^{240}Pu at 0.861 MeV with an intensity of $1.6 \times 10^{-4}\%$, while the 0^+ ground state is populated with an intensity of 76.7%. Estimate the ratio between these decay intensities from the theory of α decay and compare with the experimental value.
22. In a certain decay process, a nucleus in the vicinity of mass 240 emits α particles with the following energies (in MeV): 5.545 (α_0), 5.513 (α_1), 5.486 (α_2), 5.469 (α_3), 5.443 (α_4), 5.417 (α_5), and 5.389 (α_6). The following γ rays in the daughter nucleus are seen (energies in keV): 26 (γ_1), 33 (γ_2), 43 (γ_3), 56 (γ_4), 60 (γ_5), 99 (γ_6), 103 (γ_7), and 125 (γ_8). Construct a decay scheme from this information, assuming α_0 populates the ground state of the daughter.
23. For the decay of ^{253}Es to ^{249}Bk illustrated in Figure 8.8: (a) Estimate the intensities of the $\ell_\alpha = 0, 2, 4,$ and 6 contributions to the decay to the ground state and compare with the measured values. (b) Assuming the $\ell_\alpha = 2$ component to be dominant, estimate the relative intensities of the decays to the $\frac{9}{2}^+$ and $\frac{11}{2}^+$ states. The ground-state Q value is 6.747 MeV, and the excited states are at 42 keV ($\frac{9}{2}^+$) and 94 keV ($\frac{11}{2}^+$).
24. The decay of ^{253}Es ($I = \frac{7}{2}, \pi = +$) leads to a sequence of negative-parity states in ^{249}Bk with $I = \frac{3}{2}, \frac{5}{2}, \frac{7}{2}, \frac{9}{2}, \frac{11}{2}, \frac{13}{2}$. For each state, find the permitted values of ℓ_α .